Phantasmidine: An Epibatidine Congener from the Ecuadorian Poison Frog *Epipedobates anthonyi*[⊥]

Richard W. Fitch,* Thomas F. Spande, H. Martin Garraffo, Herman J. C. Yeh, and John W. Daly[†]

Laboratory of Bioorganic Chemistry, National Institute of Diabetes, Digestive and Kidney Diseases, National Institutes of Health, DHHS, Bethesda, Maryland 20892

The skin of the Ecuadorian poison frog *Epipedobates anthonyi* contains the potent nicotinic agonists epibatidine (**1**) and *N*-methylepibatidine (**3**). In addition, a condensed tetracyclic epibatidine congener has been identified with activity at nicotinic acetylcholine receptors, but different selectivity than epibatidine. This rigid tetracycle has been named phantasmidine (**4**). Phantasmidine has a molecular formula of $C_{11}H_{11}N_2OCl$, shares a chloropyridine moiety with **1**, and also contains furan, pyrrolidine, and cyclobutane rings. A combination of GC-MS and GC-FTIR analysis with on-column derivatization, 1D NMR spectroscopy with selective irradiation, and spectral simulation, along with 2D NMR, were used to elucidate the structure from a total sample of ∼20 µg of HPLC-purified **4** and its corresponding acetamide (**5**). After synthesis, this novel rigid agonist may serve as a selective probe for β4-contaning nicotinic receptors and potentially lead to useful pharmaceuticals.

Amphibians, in general, and poison frogs, in particular, have been a significant source of biologically active natural products.[1,2] A number of frog-skin alkaloids have been shown to have activity at nicotinic acetylcholine receptors.[3,4] The ability of poison frogs to sequester alkaloids from their diet results in a unique complexity, and to date over 800 alkaloids in more than 20 structural classes have been characterized.[1]

In 1992, epibatidine (**1**) was isolated and characterized from the frog *Epipedobates anthonyi* (formerly *Epipedobates tricolor*, Boulenger, 1899).[5] This compound has become one of the most well-studied members of the frog alkaloids due to its potent analgesic activity resulting from activation of nicotinic receptors.[6–9] However, the chemical complexity of this extract (over 80 alkaloids) has prompted the investigation of other alkaloids, including epiquinamide (**2**).[9] Although the activity initially ascribed to **2** was later found to be due to a cross-contamination artifact,[10] other compounds within this extract were also found to have nicotinic activity.[7] One was the known *N*-methylepibatidine (**3**). Another, a condensed tetracyclic alkaloid (**4**), distinctly different from the epibatidine skeleton, represents a new structural class. This novel rigid nicotinic ligand has selectivity for β4-containing nicotinic receptors, distinct from **1**. As such, **4** may serve as a useful pharmacological probe and potential lead compound for the development of selective nicotinic receptor therapeutics. We have named this compound phantasmidine after the trivial name for *E. anthonyi*, the "phantasmal poison frog".

Though promising, **4** was obtained in only microgram amounts, insufficient for full pharmacological characterization. We are currently working to synthesize **4** to confirm the structure proposed in this paper and allow full pharmacological characterization of this fascinating molecule and prepare analogues thereof. The identification, structure elucidation, and preliminary biological characterization of **4** are reported herein.
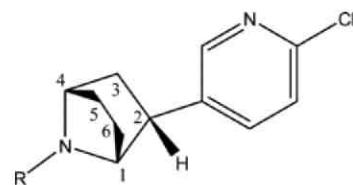
Results and Discussion

Structure Elucidation of Phantasmidine (4). Collection, preparation of alkaloid fractions, and preparative HPLC of *E.*
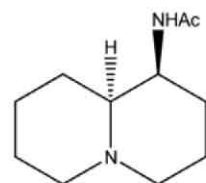

1 R = H (epibatidine)
3 R = Me

Epiquinamide (**2**)
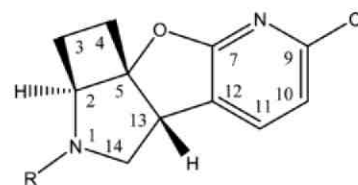
4 R = H (phantasmidine)
5 R = Me
6 R = Ac

anthonyi were performed as previously described.[9] In this extract over 80 alkaloids were found, including epibatidine (**1**). Bioassay analysis of isolated fractions in HEK cells expressing rat α3 and β4 nicotinic receptor subunits indicated at least three fractions having nicotinic-agonist activity (see Supporting Information). These included epiquinamide (**2,** with artifactual activity from cross-contamination with epibatidine),[9,10] epibatidine (with the major activity of the three),[5] and a third active fraction eluting shortly after epibatidine. Epibatidine (**1**) was the major chlorinated compound present, with molecular weight 208/210 as determined by LC-UV-APCIMS. Also present but at substantially lower concentration were two chlorine-containing congeners of isotopic molecular weight 222/224. Each had significant bioactivity. How-

* Corresponding author. Current address: Department of Chemistry and Physics, Indiana State University, 600 Chestnut St., Science S35E, Terre Haute, IN 47802. Tel: (812) 237-2244. Fax: (812) 237-2232. E-mail: Richard.Fitch@indstate.edu.
† Deceased March 5, 2008.

ever, this was incompletely resolved from that of the much more abundant epibatidine. The first alkaloid, eluting immediately prior to **1**, was determined to be the known *N*-methylepibatidine (**3**) by LC-APCIMS, GC-EIMS, and GC-CIMS comparison with authentic material.[6] Alkaloid **3** is essentially equipotent with epibatidine, and its pharmacology has been described, though this is the first detection of **3** in Nature. Though isobaric with **3**, the second alkaloid (**4**) was determined to have an exchangeable hydrogen, and its EIMS was incompatible with such a simple epibatidine derivative as **3**. Alkaloid **4** eluted shortly after **1** on LC-MS, and its UV absorption at 260 nm suggested the presence of a pyridine ring, analogous to epibatidine.

Analytical and semipreparative HPLC was conducted as described previously[9] with collection of fractions in 96-well plates and the wells sampled for assessment of nicotinic receptor activity in functional fluorescence assays in live cells using dyes sensitive to intracellular calcium levels or membrane potential (a surrogate for ionic flux).[11] Activity was assessed in several cell lines expressing various combinations of nicotinic-receptor subunits.[12–17] Comparison of the LC-MS trace with the time−bioactivity profile indicated **4** to be a nicotinic agonist (see Supporting Information). We had some initial concerns that cross-contamination by **1** might be responsible for the activity, based on previous experience in the isolation of **2**.[10] However, the relative activity of **4** did not parallel **1** across several cell lines expressing different nicotinic-receptor subtypes (see below). This observation led to the conclusion that **4** is a novel alkaloid and nicotinic acetylcholine receptor agonist with altered subtype selectivity relative to **1**.

The bulk of the initial characterization of **4** was performed by GC-MS and LC-APCI-MS during evaluation of the original extract. Additional work was done on the isolated compound, but was limited, given that only microgram quantities were present in the HPLC eluate. Nonetheless, adequate data were obtained for full characterization. The GC-CIMS (NH_3) spectrum gave the expected $[M + H]^+$ ion at *m/z* 223/225, while deuterium exchange using CI-ND_3 indicated a single exchangeable hydrogen. This was also observed with LC-APCI-MS when D_2O was used in place of H_2O in the mobile phase during the characterization of the initial extract. The GC-EIMS of **4** exhibited a molecular ion at *m/z* 222/224 and fragmentation that could generally be ascribed to α-cleavages of the three bonds adjacent to the pyrrolidine nitrogen (S1, Supporting Information).[18] There were two major complementary fragments at *m/z* 167/169 (M − C_3H_5N, base peak) and *m/z* 56 (C_3H_6N) and a third major peak at *m/z* 80. The latter peak appears to arise from facile ring expansion followed by a complex rearrangement and aromatization to afford a pyridinium ion derived from the pyrrolidine ring. Since the pyrrolidine N is lost as a neutral molecule to provide the base peak at *m/z* 167/169, the proposed fragmentation pathway requires another atom to carry the positive charge. This is possible using the oxygen atom, in which the radical ion is stabilized by the pyridine ring. Minor fragment pairs were also present at *m/z* 207/209 (M − CH_3) and *m/z* 194/196 (M − C_2H_4), the latter arising from cleavage of the cyclobutane ring with subsequent loss of ethylene. The rearrangement producing *m/z* 80 and the presence of a secondary amine were supported by co-injection of **4** with formalin−formic acid, effecting an Eschweiler−Clarke-type methylation in the 250 °C injector port to produce derivative **5**.[19,20] The mass spectrum of **5** showed the expected shift of the molecular ion to *m/z* 236/238. Also noted were shifts of the *m/z* 56 and 80 fragments in **4** to *m/z* 70 and 94, respectively, in **5**, clearly indicating the aliphatic nitrogen to be present in each fragment as a secondary amine. A key observation was the absence of the *m/z* 167/169 base peak fragment of **4** with no mass-shift equivalent in **5**. EIMS of **4** in the presence of ND_3 produced shifts of +1 amu in each of the fragments, including *m/z* 167/169. These two observations suggested that the aliphatic NH of **4** is involved in the fragmentation producing *m/z* 167/169 in a way that the methyl group

could not participate, involving the transfer of the amine H (or D when using ND_3).

Co-injection of **4** with acetic anhydride afforded *in situ* formation of acetamide **6** with parent ion at *m/z* 264/266. This gave several fragments similar to **4**, resulting from primary loss of the acetyl group as ketene to afford **4** directly. Thus, fragments at *m/z* 222/224, 167/169, 80, and 56 were present in similar proportions as with the spectrum of **4**, along with a fragment pair at *m/z* 221/223, which possibly gave rise to fragment pairs at *m/z* 193/195 and 166/168.

Although HRFABMS was attempted on **4**, only the ^{35}Cl isotope peak for $[M + H]^+$ was identified unambiguously. However, a satisfactory HREIMS value for both isotopic parent ions was obtained for the isolated acetyl derivative **6** (see below), which inferred a molecular formula of $C_{11}H_{11}N_2OCl$ for **4**. The presence of an oxygen and an additional unit of unsaturation in **4** as compared to **1** further supported the novelty of this epibatidine congener.

The vapor-phase infrared spectrum from GC-FTIR of **4** (see Supporting Information) was descriptive principally in absorptions that were missing. No C−H stretching vibrations from mono-, di-, or trisubstituted double bonds were observed, though one or more aromatic C−H (3055 cm^{-1}) and a chloropyridine with aromatic stretching absorptions (1595 and 1418 cm^{-1}) were seen, similar to those in **1**. As is common in the vapor-phase IR spectra of amines, no ν_{NH} was observed. However, mass spectrometric data and *in situ* derivatization confirmed the presence of a secondary amine. While many bands similar to **1** were observed in **4**, the prominent 1110 cm^{-1} band of **1** was missing. Comparison of the IR spectrum of **4** with those of epibatidine, 2-chloropyridine, 2-chloro-6-methylpyridine, and 2-chloro-6-methoxypyridine suggested that the oxygen could be attached to the pyridine 6-position, characterized by a band at 1264 cm^{-1}.[5,21] While not compelling evidence by itself, this structural feature was consistent with NMR data shown below, suggesting the oxygen to be adjacent to the pyridine nitrogen at C-7. Interestingly, the GC-FTIR spectrum of **4** displayed an absorption in an unusual region of the spectrum, just below 3000 cm^{-1}. The structures of the frog skin alkaloids usually contain five- and six-membered rings, and the absorptions seen in the 2900−3000 cm^{-1} region are usually below 2975 cm^{-1}. In the case of **4** the absorption at 2997 cm^{-1} is clearly due to the cyclobutane ring.[22]

NMR analysis of initially isolated **4**·DCl[23] indicated an impurity in the sample, but provided useful information. A second HPLC purification gave a cleaner sample but contained a different impurity, a not uncommon experience when working with such tiny samples. Nonetheless, consistencies in the two data sets afforded unambiguous assignments of many structural features.

The ^1H NMR spectrum of **4**·DCl in CD_3OD revealed a number of distinctive features (see Table 1 and the spectrum in the Supporting Information). In contrast to **1**, only two vicinal aromatic hydrogens were observed. Two doublets at 7.05 and 7.70 ppm indicated that the chlorine (by analogy with **1**) was on one side of the pyridine ring and two other substituents were on the opposite side. The aliphatic portion of the spectrum exhibited two spin systems, one consisting of five spins and another consisting of three spins. There were four resonances in the 3.5−4.5 ppm range. Three of these comprised a single-spin system with the hydrogen assigned as H-13 showing benzylic coupling to H-11 and a methylene (assigned by COSY) adjacent to a heteroatom, which we assigned as the secondary ammonium group. While this is technically a five-spin system because of the benzylic coupling, we consider it here as a three-spin system and a separate two-spin system for simplicity. The remaining midfield signal at 4.24 ppm was part of a five-spin system and was coupled to two consecutive methylenes. We assigned this to a cyclobutane system on the basis of COSY data and the observation that the methylene protons were highly nonequivalent and tightly coupled, and the system terminated at a quaternary center, as all four signals were at 2.5 ppm or below.

Table 1. NMR Data for **4** and **6** (500 MHz, CD$_3$OD)

	phantasmidine (**4**)			*N*-acetylphantasmidine (**6**)		
position	δ_H (*J* in Hz)	δ_C (ppm)^a (major/minor)	δ_H (*J* in Hz) major rotamer	δ_H (*J* in Hz) minor rotamer	1D irradiation at #H affects	
2	4.24 (dd, 7.5, 7.0)	65	4.70 (dd, 7.56, 6.31)	4.79 (dd, 7.56, 6.93)	2→3α, 3β, 4β; 2′→3α′, 3β′, 4β′	
3α	2.22 (qd, ~11, ~3.4−7.1)	20	2.45 (ddd, 3.2, 8.0, 11.3)	2.39 (m)	^{b}	
3β	1.74 (m)		1.69 (dtd, 6.2, 9.3, 12.0)	1.62 (m, 6.5, 8.6)	^{b}	
4α	2.63 (q, 11.5)	27.5	2.53 (m, 0.6, ~2, ~11)	2.55 (m, 0.4, 1.5, ~11)	^{b}	
4β	2.38 (t, 11.9)		2.37 (m)	2.35 (m)	^{b}	
10	7.02 (d, 7.7)	118.5	6.99 (d, 7.69)	7.01 (d, 7.69)	10,10′→11, 11′	
11	7.70 (bd, 7.7)	138.3	7.69 (dd, 7.69, 1.0)	7.72 (dd, 7.66, 1.2)	11, 11′→10, 10′	
13	4.08 (bd, 6.8)	48.4/49.4	4.08 (m)	4.15 (ddd, 8.2, 2.8, ~1)	13 →14α, 14 β; 13′→14α′, 14 β′	
					13, 13′→11, 11′ (small *J* removed)	
					13, 13′→3β, 3β′	
14α	3.92 (bt, 7.2)	53.2/54.6	4.08 (m)	3.96 (dd, 11.6, 3.2)	14 α′→14 β′, 13′;14α→ 14 β, 13	
14β	3.69 (bd, 12.5)		4.02 (dd, 7.0, 16.2)	4.32 (dd, 11.6, 8.3)	14 β→3 β	
Ac		21.6 (CH$_3$)	2.01 (s)	2.00 (s)		

^{a} Determined from HMQC data. ^{b} Discussed in more detail in the text.

The HMQC spectrum of **4** was acquired with the early impure material but gave no conclusive data due to the small sample size and impurities present. By analogy with **1**, the chlorine was assigned to C-9 adjacent to the pyridine nitrogen. It was anticipated that the biosynthetic pathway for this unusual function would be analogous to that of **1**, suggesting that the position of the chlorine would be conserved in any related metabolites. The remaining two substituents on the pyridine ring were assigned as a furan ring on the basis of two lines of NMR evidence. First, the previously mentioned benzylic coupling of the broader 7.70 ppm doublet to another doublet resonance at 4.08 ppm was revealed by the COSY spectrum, indicating a carbon substituent with a benzylic hydrogen at that position. Second, an ether oxygen was required for the structure, as an alcohol was ruled out due to the absence of OH bands in the GC-FTIR spectrum. The assignment of the single exchangeable hydrogen to a secondary amine was made on the basis of *in situ* methylation[20] and acetylation in the GC-MS injector. Oxygenation at C-7 was also inferred from comparison of the IR spectrum of 2-chloro-6-methoxypyridine,[21] which bears a significant similarity to that of **4**.

Acetylation of **4** by treatment with excess acetic anhydride and evaporation under nitrogen afforded isolable **6** for analysis by ^{1}H NMR spectroscopy. This gave approximately 20 μg of **6**, the amount determined by adding a known quantity of CHCl$_3$ to the CD$_3$OD NMR sample. Acetamide **6** was clearly distinct from *N*-acetylepibatidine[5] by MS and NMR. HRMS analysis of the isotopic molecular ions at *m/z* 264 and 266 indicated a molecular formula of C$_{13}$H$_{13}$N$_2$O$_2$Cl (see Experimental Section), which also established the molecular formula of **4** by difference. The EIMS fragments for **6** at *m/z* 179, 167, and 80 were mass measured and their formulas determined to be C$_9$H$_6$NO^{35}Cl, C$_8$H$_6$NO^{35}Cl, and C$_5$H$_6$N, respectively. As noted above, these fragments were present in similar proportions as with the spectrum of **4**, thus supporting the assignment of the fragmentations noted for **4** (S1, Supporting Information).

A major and a minor rotamer were observed in a 2:1 ratio in the ^{1}H NMR spectrum of **6**, complicating interpretation, particularly in the aliphatic region. Nonetheless, the spectrum provided further evidence for the assignments of some hydrogens, aided by 1D decoupling experiments as well as by the 2D TOCSY (with variable mixing times) and HMQC spectra. Notably, H-14α, H-14β, and H-2 were shifted downfield in the ^{1}H NMR spectrum, due to the acetyl group. The greatest challenge was in the assignment of the cyclobutane resonances, since overlapping signals for the major and minor rotamers produced significant congestion. The signal for H-2 was cleanly related to protons H-3α and H-3β by a TOCSY experiment with a short mixing time (5 ms), while a longer time (30 ms) elaborated H-4α and H-4β. This was also visible for the minor rotamer, but the weak signals made precise assignment difficult. However, selective 1D irradiation of the known multiplets

facilitated several assignments as shown in Table 1. Key to the final assignment was the fact that H-3β was observed at unusually high field (1.68/1.60 ppm for major/minor rotamers, respectively) for a cyclobutane proton, while H-3α was seen at lower field (2.44/ 2.37 ppm for major/minor rotamers, respectively). This was consistent with the HMQC spectrum, though the two cross-peaks were quite weak, which can be explained on the basis that H-3β projects into the shielding cone above the acetamide π-system[24] and is consistent with molecular models (Chem3D). Protons H-4α (2.35/2.34 ppm) and H-4β (2.47/2.48 ppm) were much closer together, lacking this influence, and were found at chemical shifts more consistent with cyclobutanes.[25] TOCSY spectra were particularly helpful for sorting out the minor rotamer shifts on the basis of cross-peaks from the resonance of H-3β, since the rotamers were well-separated. The two aromatic hydrogens were present in a 2:1 ratio of major/minor rotamers, with the major rotamer being upfield for both signals. The most downfield proton for H-11 at 7.70 ppm was observed as a doublet of doublets (*J* = 7.7, 1.0 Hz), and long-range coupling to H-13 was observed using 1D decoupling (see Table 1), consistent with **4**. An incomplete HMQC spectrum was obtained for **6**, with several weaker signals missing, principally those of the minor rotamer. Nonetheless, several useful correlations were seen that aided in structure elucidation. These included the observation that the five-spin system, comprising the remainder of the proton spectrum, arose from protons on three carbons. A portion of this system was present as a complex pattern of overlapping multiplets in the region of ca. 2.3−2.6 ppm and was derived from three protons on two carbons (H-3α and H-4α, H-4β). The remainder of this system was another group of overlapping multiplets at 1.6−1.8 ppm, which was derived from a proton on a single carbon (H-3β, both rotamers).

To aid interpretation of the complex multiplets, the five-spin system of **6** was simulated at 600 MHz (Bruker NMR-SIM, see Supporting Information) based on isolating the H-4β signal and its couplings and using those with the assignments made for the other four protons, H-2 to H-4, of **6**. Likewise, the three-spin system of H-13, H-14α, and H-14β of **6** was simulated, and coupling constants were extracted (see Supporting Information). The three-spin system comprised two sets of three signals, one ascribed to the major rotamer, the other to the minor rotamer (indicated with the *prime* (′) notation). The minor rotamer was seen clearly with well-separated protons, each appearing as a doublet of doublets, having two vicinal couplings and one geminal coupling (see Table 1). The major rotamer was more complex, yielding a second-order spectrum with H-13 overlapping H-14β and appearing as two triplets with H-14α appearing slightly upfield as a doublet of doublets. The overlap of H-13 and H-14β was shown by the carbon signals at 48.4 and 53.2 ppm for the proton multiplet at 4.07−4.12 ppm. The three-spin simulation with applied J_{AB} = 9, J_{AC} = 3, and J_{BC} = 11.8 Hz was virtually identical to the acquired ^{1}HNMR spectrum

of **6** at 600 MHz (see Supporting Information). Selective 1D decoupling independently confirmed these two three-spin systems and allowed coupling constants for the minor rotamer to be determined (see Table 1). In both the minor rotamer and major rotamer, H-13 had a long-range coupling (ca. 1 Hz) with the most downfield doublet at 7.73 ppm, which was removed by irradiation at the position of H-13′ (4.15 ppm) or H-13 (4.08 ppm), respectively. Molecular modeling (MM2, Chem3D) indicated a dihedral angle between H-13 and H-11 of 117°, making the benzylic C−H bond nearly parallel to the π-system, affording efficient coupling.[26]

The rotamer effect on H-4 was minimal. Thus, H-4α and H-4α′, each a triplet of doublets, overlapped, giving an apparent quartet of doublets. Slightly upfield of this multiplet was a complex multiplet (2.32−2.44 ppm) that 1D decoupling indicated to be from H-3α, H-4β, H-4β′, and H-3α′, with the latter three signals upfield of H-3α. This unfortunate coincidence of three signals made interpretation difficult for this region of the proton spectrum. The most upfield multiplet (1.58−1.75 ppm) of the five-spin system included signals assigned to H-3β and H-3β′, with the minor rotamer separated nicely as a multiplet at 1.58−1.62 ppm. As Table 1 indicates, irradiation at H-2 and H-2′ removed a small *J* value from H-4β and H-4β′, indicating a long-range coupling between the H-2 and H-4β protons, whereas H-4α and H-4α′ in **4** were unaffected. Such long-range coupling is not uncommon in rigid systems such as bicyclic terpenes, many with a four-membered ring as part of the structure, where a four-bond coupling is often observed.[27] Also on irradiation at H-2, a medium-sized *J* value was removed from H-3β and an apparent quartet with *J* ≈ 10 Hz resulted. Irradiation at H-2′ had a similar effect on H-3β′. Irradiation at H-2 and H-2′ also affected the H-3α and H-3α′ signals, respectively, removing a medium *J* value from each.

The COSY spectrum showed a number of useful cross-peaks that were consistent with 1D decouplings, but the resolution was such that unambiguous assignments were limited. A weak cross-peak was observed for another long-range coupling between H-14β and H-3β. The spectrum also indicated the multiplet between 2.42 and 2.45 ppm to be from a single proton (H-3α), showing coupling with H-3β but not with H-3β′, and which was cleanly separated at 600 MHz. Other couplings were observed for the five-spin system, but were complicated by the overlap of H-4α with H-4α′ and a combined overlap of H-3α′, H-4β, and H-4β′. However, 1D decoupling was of significant utility. Irradiation at H-3β again showed the multiplet assigned to H-3α to be a single proton. The reverse decoupling showed the multiplet for H-3β (1.66−1.73 ppm) also to be from a single proton. A large *J* value was removed in either case judged by the decrease in the width of the multiplets. Irradiation at H-3β removed a large *J* value from H-2, whereas irradiation at H-3α removed a smaller coupling.

The unusual separation between H-3α and H-3β (Δ = 0.75 ppm) in **6** may be suggested as being due to the shielding effect of the acetamide carbonyl. However, a similar but smaller effect for H-3 protons (Δ = 0.48 ppm) was seen with the amine **4**, which lacks this function. A much smaller effect (Δ = 0.16 ppm) was seen with the H-4 protons in both **4** and **6**. In both cases, it is the β-protons that are shielded, which would suggest an effect from the pyrrolidine nitrogen.

The TOCSY spectrum (30 ms mixing time) showed no coupling between H-3α and H-3β′, clearly indicating that each multiplet belonged to separate molecules. Cross-peaks between the H-4α/H-4α′ overlapping multiplet (2.5−2.6 ppm) and the slightly separated signals for H-3β (1.66−1.71 ppm) and H-3β′ (1.64−1.58 ppm) confirmed their respective connectivities. The same TOCSY spectrum showed cross-peaks between H-2 and H-3α, H-3β, H-4α, and H-4β, all of roughly equal intensity. The three-spin system of the minor rotamer was seen clearly with cross-peaks between H-13′, H-14α′, and H-14β′. The three-spin system of the major rotamer

showed only one cross-peak, as H-13 and H-14α overlapped but did correlate with H-14β.

On the basis of these data, we postulate the structure for **4** as shown. The chloropyridine is consistent with NMR and IR data and analogous to **1**. Exchange and derivatization data demonstrated the presence of a secondary amine, again consistent with **1**. HRMS indicated a single oxygen, for which other data suggested an ether. If the amine is taken to be part of a pyrrolidine system as present in **1**, this leaves two rings remaining, as no double bond is evident in the proton NMR spectrum. This can be achieved by closure of one ring with the oxygen terminus and pyrrolidine β-carbon, while fusing a cyclobutane with the same pyrrolidine β-carbon and α-carbon, producing a condensed tetracycle with a central quaternary center. Molecular modeling of this tetracycle rules out many possible orientations of the oxygen, H-2, and H-13. The structure as shown, having H-13 on the β-face and the oxygen and H-2 on the α-face, most closely approximates the calculated dihedral bond angles (θ) and the H−H couplings observed with **4** and **6** (see below). This is also consistent with two of the C−H orientations (H-2, H-4) seen in **1**, as though **4** might be biosynthetically derived from **1** or a common precursor. It appears that migration of the C-1 to C-6 bond in **1** with new bond formation between C-6 and C-3 (C-4 and C-5 in **4**) could generate this novel ring system. However, this is only speculative and the role of the oxygen is not clear. The absolute configuration of **4** is not known, but is likely to be that shown. Natural **1** has the (1R,2R,4S) configuration as shown, and **4** would be expected to have the *R*-configuration at C-13 by analogy.

The junctions between the furan, cyclobutane, and pyrrolidine rings were assigned as *cis*, since a *trans*-fusion would be ~18 kcal/mol higher in energy and also incompatible with the observed couplings based on molecular models (Chem3D). The model of **4** (with configuration as shown) indicates a dihedral angle of ~15° between H-13 and H-14β, which would give a vicinal $^3J_{AB}$ of ~7 Hz. Likewise, the dihedral angle between H-13 and H-14α is calculated to be ~104°, affording a small $^3J_{AC}$ of ~2 Hz or less. The corresponding *trans*-fused isomer (with H-13 on the α-face) would have values of 167° and 44° for these respective dihedral angles. This would require larger *J* values of 10 and 4 Hz, respectively, such that neither H-13 nor H-14α could appear as simple doublets, as is observed in the ^{1}H NMR spectrum of **4**. The observed *J* values of 12.5 Hz (geminal ^2J, H-14α−H-14β) and 6.8 Hz ($^3J_{AB}$, H-14β--H-13) are therefore consistent with the depicted *cis*-geometry.

2D-TOCSY and COSY correlation spectra and HMQC data are consistent with the proposed structure, although 1D decoupling provided greater insight into the structure because of overlaps that obscured some 2D data of **6**. Due to the small sample size, a NOESY required 60 h but did show the acetamide methyl correlated with H-2 in the major rotamer and with H-14β′ and H-14α′ in the minor rotamer (see Figure 1 and the corresponding spectrum in the Supporting Information). Another key nonscalar cross-peak observed at 600 MHz was that of H-4β with H-13, again supporting the relative stereochemistry of both ring junctions as *cis*.

Biological Investigation of Phantasmidine. Semipreparative HPLC-bioassay analysis was conducted as described previously[9] on the alkaloid fraction of *E. anthonyi* in several cell lines, including TE-671 (neuromuscular),[16] SH-SY5Y (ganglionic α3*, α3β4*, α7),[15] and several transfected cell lines expressing nicotinic-receptor subunit combinations of α2−4 and β2/β4 (see Experimental Section).[12,13,17]

The separated fractions afforded several activities at various times depending on the cell line examined (see Supporting Information), although most of the agonist activity was limited to the early (5−20 min) range. Epibatidine (**1**)[5] was easily identified by APCI-MS at 13.25 min and was active in all cell lines to varying degrees, with the greatest activity being in cells transfected with α3 and β4
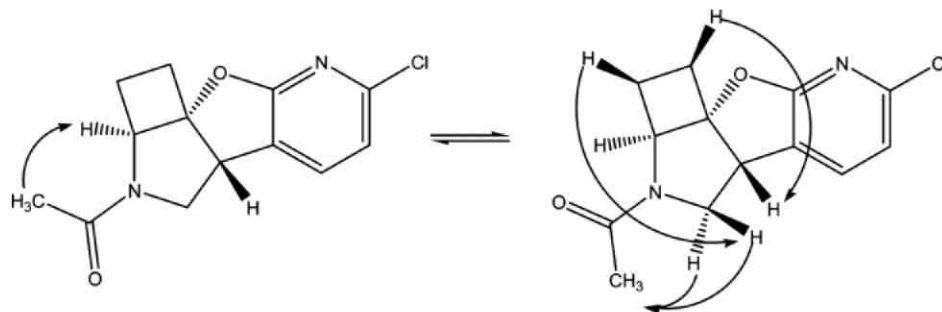
Figure 1. Key NOE correlations for **6**.

subunits. This is consistent with the known pharmacological profile of epibatidine.[8,10,13] Epiquinamide (**2**)[9] was identified at 6 min, although its activity was later found to be an artifact due to a cross-contamination from **1**.[10] The relative activity of **2** across the various cell lines was also consistent with that of **1**. A third major area of activity was found at 15 min and corresponded to an APCI-MS peak at 15.2 min having *m/z* 222/224. Initially it was thought to be a methylepibatidine, and indeed, *N*-methylepibatidine (**3**) was identified by APCI-MS at 13 min, being confirmed by comparison with previously synthesized material.[7] Compound **3** was responsible for the leading edge of the epibatidine activity in the bioassay profile. However, the third activity was clearly not a methylated epibatidine, as HRMS indicated the presence of an oxygen and an additional unit of unsaturation. Consequently, the alkaloid, named phantasmidine, was isolated and its structure (**4**) determined as described above.

On the basis of the previous observation that epiquinamide was incorrectly assigned activity due to contamination of the fractions with the very potent epibatidine,[10] we initially had concerns that the activity of **4** might be due to similar contamination. These were allayed by the careful observation of the relative activity of **4** as compared to **1** based on the height and area of the activity peaks. Eluting at 13.25 min, **1** consistently displayed the greatest activity in the sample regardless of cell line examined. The activity initially ascribed to **2** at 6 min was of consistent relative size in each cell line, supporting cross-contamination by **1** as the likely explanation for its activity. However, **4**, which eluted at 15.20 min, showed higher relative activities in cell lines expressing β4 nicotinic subunits (KXα3β4R2,[12] KXα4β4R1,[13] IMR-32,[14] SH-SY5Y[15]) and less activity in neuromuscular (TE-671[16]) and β2-containing (KXα4β2R2,[13] K-177[17]) cells. This suggested that **4** has an altered selectivity relative to **1** and may, like **1**, find use as a pharmacological probe.

There are significant differences in the pharmacological profile between β2- and β4-expressing cells.[28] Much interest has been displayed in nicotinic agonists having selectivity for β2-containing receptors (principally α4β2). These receptors have been implicated as targets for analgesia, cognition, and smoking cessation.[29–32] A substantial number of ligands have been developed with β2-selectivity. However, at present there are few β4-selective nicotinic agonists. Norchloroepibatidine and UB-165 display only a modest (3–10-fold) β4 preference over β2, while AR-R17779 is more selective (>20-fold), though the latter is considered a selective α7 agonist.[4,33,34] Mice in which the β4-subunit has been knocked out are resistant to nicotine-induced seizures and exhibited reduced nicotine withdrawal relative to their wild-type counterparts.[35,36] A highly rigid β4-selective agonist such as **4** may provide a useful tool for probing subtype-selectivity in this receptor class. Like many receptors, high-potency, subtype-selective nicotinic-receptor agonists are rare, though antagonists are more common. While antagonists need only bind to the receptor, the additional structural requirements for activation of receptors make the design of agonists more demanding. Derivatives of **4** may serve as useful pharmacologic probes for β4-containing nicotinic receptors, much as the

semirigid laburnum alkaloid cytisine[31] and pyridohomotropane (a derivative of the dinoflagellate alkaloid anatoxin)[37,38] have for β2-containing receptors. Cytisine has been used extensively as a probe for α4β2 receptors in natural and radiolabeled[39] forms for *in vitro* pharmacology as well as clinically as a smoking cessation agent,[31] where the drug varenicline (Chantix, Pfizer) is an analogue of cytisine.[31] We are also quite interested in the potential of **4** and analogues at α7 and/or 5-HT₃ receptors given its structural similarity to pyridofurans currently under investigation by Lilly[40–43] and Astra Zeneca.[44]

The N−N distance in **4** is calculated to be approximately 5.1 Å (MM2, Chem3D), consistent with the currently proposed nicotinic pharmacophore of epibatidine.[45–47] It is representative of an epibatidine conformation in which the chloropyridine ring is essentially coplanar with C-5 and C-13, which comprise the proximal bridge of the azabicycle (see Figure F1 in the Supporting Information). Subtle, but perhaps significant differences in the vector orientation of potential H-bonding sites at the two nitrogens can be observed, which may contribute to the observed selectivity.[46]

Nicotinic receptors are the prototypical ligand-gated ion channels, and their function is critical to fast synaptic transmission in the central nervous system.[48] While much has been learned about their function, more remains to be learned in order to tease out their roles in disease and normal physiology. Natural products have played a critical role in the characterization of nicotinic receptors.[3] New selective ligands are needed to characterize the more than 15 known subtypes of these receptors for both biological and pharmacological study.[49] Phantasmidine (**4**) may fill a new niche for characterization of β4-containing nicotinic receptors. However, as natural **4** is not available in sufficient quantity for detailed pharmacologic analysis, we are currently engaged in the synthesis of **4** as well as some simple analogues. This will allow us to confirm its structure and activity as well as establish the pharmacology and subtype-selectivity across the known nicotinic-receptor subtypes, with the goal of determining basic structure−activity relationships.

Experimental Section

General Experimental Procedures. Reagents and solvents used were of ACS reagent or HPLC grades and were used as received. NMR analysis was performed on Varian Inova 500 MHz and Bruker Avance II 600 MHz spectrometers. Chemical shifts (δ) are reported in ppm relative to TMS, and coupling constants (*J*) are reported in Hz. GC-MS was conducted using a Finnigan GCQ in EI and CI (NH₃ or ND₃) modes using an RTX-5MS column (25 m × 0.25 mm i.d.) and a temperature program of 100 °C held for 1 min followed by a ramp to 280 °C at 10 °C/min, then held at 280 °C for 10 min. GC-FTIR spectra were acquired using a Hewlett-Packard 5890 GC (same column except 0.32 mm i.d., same temperature program) interfaced with a narrow band 5965B infrared detector. HPLC-MS was performed using an Agilent 1100 binary HPLC system interfaced with a Finnigan LCQ ion trap mass spectrometer. Molecular modeling was performed using Chem3D Pro (v. 8.0, Cambridge Scientific Computing, Cambridge, MA). NMR spectral simulations were performed using NMRSIM (Bruker, v. 4.3).

Animal Material and Initial Processing. Collection of specimens of *Epipedobates anthonyi* (formerly *E. tricolor*), preparation of extracts, and HPLC separation were essentially as described previously.[9] Briefly,

the alkaloid fraction from the methanolic extract of 183 skins (net 6 mL at 13 g skin/mL) was analyzed by HPLC-UV-MS using a Phenomenex Aqua 125 Å C_{18} column (4.6 × 250 mm) and a gradient of H_2O/CH_3CN, with each component containing 0.1% HOAc, from 90% to 50% H_2O over 40 min and held 10 min. For biological analysis, otherwise identical runs were conducted with only UV detection and collection of the eluate into 96-well plates covering the interval of 4 to 64 min using an Isco Foxy 200 fraction collector. The collected fractions were acidified with HCl to suppress alkaloid volatility and evaporated under nitrogen flow. The plate was sealed with parafilm and kept at −20 °C until use.

Bioassay. Collected analytical-scale fractions in 96-well plates were reconstituted *in situ* with 300 μL of Hanks balanced salt solution containing 20 mM HEPES at pH 7.4 (HBSS/HEPES) and were used as such. Cell lines expressing various nicotinic receptors were maintained in culture and used for functional fluorescence assays including SH-SY5Y, IMR-32, TE-671, KXα3β4R2, KXα4β4R1, and KXα4β2R2, as previously described.[9,11] Briefly, cells were plated onto 96-well poly-D-lysine-coated plates in Dulbecco's modified minimum essential media supplemented with 10% fetal bovine serum (supplemented with Geneticin G418 for KXα3β4R2, KXα4β4R1, and KXα4β2R2 cells) and grown to near confluence. The media was aspirated and the cells were gently washed with 2 × 100 μL of HBSS/HEPES (pH 7.4). A solution of Molecular Devices no-wash membrane potential dye (30 μL) was added, and the cells were incubated in the dark at room temperature for 1 h. Plates were read on a Flexstation (Molecular Devices) robotic plate reader at an excitation wavelength of 530 nm and emission wavelength of 565 nm, with a cutoff filter at 550 nm. Basal fluorescence was measured for 15 s, and 30 μL of reconstituted *E. anthonyi* fraction in HBSS/HEPES was added. Response was measured for 105 s, and 30 μL of 300 μM nicotine was added. The nicotine response was measured for 40 s, and 30 μL of 160 mM KCl was added. Maximal fluorescence was measured for 40 s. Average basal fluorescence was subtracted, and response was taken as the peak fluorescence for each addition divided by the maximal KCl fluorescence. Responses for each fraction were plotted as a function of time and compared to the UV and total ion chromatograms to identify active components. Preparative-scale isolation was then conducted, and structures of active components were elucidated.

Isolation of Phantasmidine (4). Preparative isolation was conducted as previously described.[9] Briefly, 5 mL of the extract was concentrated under a nitrogen flow to ~0.3 mL and separated by HPLC in a similar fashion with collection in deep-well polypropylene plates using a Phenomenex Aqua 125 Å C_{18} column (10 × 250 mm) at 2.0 mL/min with collection of fractions at 0.25 min intervals over six injections. Fractions of this eluate, found to contain **4**, were collected and analyzed by LC-APCI-MS, GC-MS in EI and CI (NH_3, ND_3) modes, GC-FTIR, and microprobe NMR (500 MHz). The initially collected fractions were found to be insufficiently pure for unambiguous NMR analysis and were rechromatographed as above. This provided material that was slightly impure, but allowed unambiguous identification of the NMR signals belonging to **4**.

Phantasmidine (4). *E. anthonyi* alkaloid extract LC peak, t_R 15.20 min, GC peak, t_R 14.66 min: UV (LC CH_3CN/H_2O, 0.05% HOAc) λ_{max} 260 nm; IR (vapor) ν_{max} 2997, 2960, 2846, 1595, 1418, 1309, 1264, 1217, 1111, 1079, 1041, 931, 810 cm^{-1}; ^{1}H NMR (500 MHz, CD_3OD) δ 7.70 (1H, d, $J = 7.7$, <1 Hz, H-11), 7.02 (1H, d, $J = 7.7$ Hz, H-10), 4.24 (1H, dd, $J = 7.5$, 7.1 Hz, H-2), 4.08 (1H, br d, $J = 6.8$ Hz, H-13), 3.92 (1H, br t, $J = ~7.2$ Hz, H-14α), 3.69 (1H, br d, $J = 12.5$ Hz, H-14β), 2.63 (1H, q, $J = 11.5$ Hz, H-4α), 2.38 (1H, t, $J = 11.9$ Hz, H-4β), 2.22 (1H, app qd, $J = 3.4$, 11.5 Hz, H-3α), 1.74 (1H, m, H-3β); EIMS *m/z* 224 (7), 223 (3), 222 (20), 221 (7), 209 (2), 207 (6), 196 (3), 194 (8), 193 (4), 181 (2), 179 (4), 169 (34), 167 (100), 131 (5), 130 (4), 80 (89), 56 (46); EIMS (with trace ND_3, major peaks only) *m/z* 170 (30), 168 (91) (one exchange), 130 (7, no exchange), 81 (100), 57 (67); EIMS/MS on *m/z* 167 *m/z* 152 (3), 149 (167 − H_2O, 17), 138 (167 − CH=O, 100), 131 (167 − H^{35}Cl, 24), 113 (167 − H_2O − H^{35}Cl, 59), 104 (167 − 63, 52); CIMS (NH_3) *m/z* 223 (100), 225 (32); CIMS/MS (on *m/z* 223) 223 (M + H, 32), 206 (M + H − NH_3, 44), 195 (M + H − C_2H_4, 100), 194 (46), 188 (36), 187 (43), 169 (11), 160 (20), 159 (38), 143 (15), 132 (20); CIMS/MS (on *m/z* 225) 225 (M + H, <5), 224 (40), 223 (22), 208 (M + H − NH_3, 22), 207 (19), 197 (M + H − C_2H_4, 100), 196 (66), 190 (32) 187 (52), 169 (22), 161 (25), 160 (34), 159 (25), 143 (14), 132 (15); HRFABMS *m/z* 223.0650 (calcd for $C_{11}H_{12}N_2O^{35}Cl$, 223.0638).

N-Methylphantasmidine (5). Co-injection of **4** with formalin and formic acid[19] afforded *in situ* methylation to give **5**: GC-MS showed t_R 14.28 min; EIMS *m/z* 238 (3), 236 (11), 223 (2), 221 (5), 210 (2), 208 (7), 195 (3), 193 (10), 181 (4), 179 (11), 168 (5), 166 (12), 94 (100), 70 (34).

N-Acetylphantasmidine (6). Co-injection of **4** with acetic anhydride afforded *in situ* acetylation to give **6**. GC-MS showed a single peak, t_R 17.82 min; IR (vapor) ν_{max} 2959, 1693, 1598, 1418, 1260, 1233, 1086, 935, 764 cm^{-1}; NMR data are given in Table 1; EIMS *m/z* 266 (25), 264 (75), 251 (6), 249 (21), 224 (14), 222 (43), 209 (8), 207 (30), 205 (23), 196 (11), 194 (36), 181 (47), 179 (63), 169 (33), 167 (100), 165 (50), 140 (5), 138 (9), 131 (4), 130 (19), 104 (9), 102 (17), 84 (20), 80 (89), 75 (10), 56 (42); HREIMS *m/z* 264.0673 (calcd for $C_{13}H_{13}N_2O_2^{35}Cl$, 264.0666), 266.0642 (calcd for $C_{13}H_{13}N_2O_2^{37}Cl$, 266.0636), 179.0142 (calcd for $C_9H_6NO^{35}Cl$, 179.0138), 167.0126 (calcd for $C_8H_6NO^{35}Cl$ 167.0132), 80.0500 (calcd for C_5H_6N, 80.0500). To a partially evaporated methanolic residue of **4** was added excess acetic anhydride, and the mixture was allowed to stand overnight, followed by evaporation of excess anhydride under nitrogen flow to afford **6**.

Supporting Information Available: HPLC and bioactivity traces, GC-FTIR, and mass spectral fragmentations for **4**, ^{1}H and 2D NMR spectra for **4** and **6**. This material is available free of charge via the Internet at http://pubs.acs.org.

References and Notes

(1) Daly, J. W.; Spande, T. F.; Garraffo, H. M. *J. Nat. Prod.* **2005**, *68*, 1556–1575.
(2) Daly, J. W. *J. Med. Chem.* **2003**, *46*, 447–452.
(3) Daly, J. W. *Cell. Mol. Neurobiol.* **2005**, *25*, 513–552.
(4) Jensen, A. A.; Frolund, B.; Liljefors, T.; Krogsgaard-Larsen, P. *J. Med. Chem.* **2005**, *48*, 4705–4745.
(5) Spande, T. F.; Garraffo, H. M.; Edwards, M. W.; Yeh, H. J. C.; Pannell, L.; Daly, J. W. *J. Am. Chem. Soc.* **1992**, *114*, 3475–3478.
(6) Badio, B.; Garraffo, H. M.; Spande, T. F.; Daly, J. W. *Med. Chem. Res.* **1994**, *4*, 440–449.
(7) Badio, B.; Shi, D.; Garraffo, H. M.; Daly, J. W. *Drug Dev. Res.* **1995**, *36*, 46–59.
(8) Dukat, M.; Glennon, R. A. *Cell. Mol. Neurobiol.* **2003**, *23*, 365–378.
(9) Fitch, R. W.; Garraffo, H. M.; Spande, T. F.; Yeh, H. J. C.; Daly, J. W. *J. Nat. Prod.* **2003**, *66*, 1345–1350.
(10) Fitch, R. W.; Sturgeon, G. D.; Patel, S. R.; Spande, T. F.; Garraffo, H. M.; Daly, J. W.; Blaauw, R. H. *J. Nat. Prod.* **2009**, *72*, 243–247.
(11) Fitch, R. W.; Daly, J. W.; Kellar, K. J.; Xiao, Y. *Proc. Natl. Acad. Sci. U.S.A.* **2003**, *100*, 4909–4914.
(12) Xiao, Y.; Meyer, E. L.; Thompson, J. M.; Surin, A.; Wroblewski, J.; Kellar, K. J. *Mol. Pharmacol.* **1996**, *54*, 322–333.
(13) Xiao, Y.; Kellar, K. J. *J. Pharmacol. Exp. Ther.* **2004**, *310*, 98–107.
(14) Lukas, R. J. *J. Pharmacol. Exp. Ther.* **1986**, *265*, 294–302.
(15) Lukas, R.; Norman, S.; Lucero, L. *Mol. Cell. Neurosci.* **1993**, *4*, 1–12.
(16) Lukas, R. J. *J. Neurochem.* **1986**, *46*, 1936–1941.
(17) Gopalakrishnan, M.; Monteggia, L. M.; Anderson, D. J.; Molinari, E. J.; Piattoni-Kaplan, M.; Donnelly-Roberts, D.; Arneric, S. P.; Sullivan, J. P. *J. Pharmacol. Exp. Ther.* **1996**, *276*, 289–297.
(18) The postulated MS fragmentations were considered after the structure was proposed with help from the NMR spectra.
(19) Brewer, A. R. E. In *Name Reactions for Functional Group Transformations*; Li, J. J., Corey, E. J., Eds.; Wiley and Sons: Hoboken, NJ, 2007; Chapter 2, pp 86–92.
(20) Daly, J. W.; Ware, N.; Saporito, R. A.; Spande, T. F.; Garraffo, H. M. *J. Nat. Prod.* **2009**, *72*, 1110–1114.
(21) Pouchert, C. J. *Aldrich Library of FT-IR Spectra: Vapor Phase*, Vol. 3; Aldrich Chemical Co.: Milwaukee, WI, 1989; p 1531A.
(22) Nyquist, R. A. *Interpreting Infrared, Raman, and Nuclear Magnetic Resonance Spectra*; Academic Press: San Diego, 2001; Vol. 1, pp 35, 48, 49.
(23) Following HPLC, the fractions were acidified with HCl to suppress volatility; thus the spectra of **4** are of the corresponding DCl salt on exchange with CD_3OD.

(24) Ring current effects are a common explanation for such effects (e.g., Pople, J. A.; Schneider, W. G.; Bernstein, H. J. *High-Resolution Nuclear Magnetic Resonance*; McGraw-Hill: New York, 1959). However, this has recently been challenged on the basis of computational data. See: Wannere, C. S.; Schleyer, P. V. R. *Org. Lett.* **2003**, *5*, 605–608.

(25) Silverstein, R. M.; Webster, F. X.; Kiemle, D. *Spectrometric Identification of Organic Compounds*, 7th ed.; Wiley and Sons: New York, 2005; Chapter 3, pp 192–193.

(26) Lambert, J. B.; Mazzola, E. *Nuclear Magnetic Resonance Spectroscopy: An Introduction to Principles, Applications and Experimental Methods*; Pearson Prentice Hall: Upper Saddle River, NJ, 2004; Chapter 4, pp 112–115.

(27) Jackman, L. M.; Sternhell, S. *Applications of Nuclear Magnetic Resonance Spectroscopy in Organic Chemistry*, 2nd ed.; Pergamon Press: New York, 1969; Vol. 5, Table 4-4-6, p 336.

(28) Parker, M. J.; Beck, A.; Luetje, C. W. *Mol. Pharmacol.* **1998**, *54*, 1132–1139.

(29) Decker, M. W.; Reuter, L. E.; Bitner, R. S. *Curr. Top. Med. Chem.* **2004**, *4*, 369–384.

(30) Sacco, K. A.; Bannon, K. L.; George, T. P. *J. Psychopharmacol.* **2004**, *18*, 457–474.

(31) Etter, J. F.; Lukas, R. J.; Benowitz, N. L.; West, R.; Dresler, C. M. *Drug Alcohol Depend.* **2008**, *92*, 3–8.

(32) Jorenby, D. E.; Hays, J. T.; Rigotti, N. A.; Azoulay, S.; Watsky, E. J.; Williams, K. E.; Billing, C. B.; Gong, J.; Reeves, K. R. *J. Am. Med. Assoc.* **2006**, *296*, 56–63.

(33) Avalos, M.; Parker, M. J.; Maddox, F. N.; Carroll, F. I.; Luetje, C. W. *J. Pharmacol. Exp. Ther.* **2002**, *302*, 1246–1252.

(34) Sharples, C. G. V.; Kaiser, S.; Soliakov, L.; Marks, M. J.; Collins, A. C.; Washburn, M. S.; Wright, E.; Spencer, J. A.; Gallagher, T.; Whiteaker, P.; Wonnacott, S. *J. Neurosci.* **2000**, *20*, 2783–2791.

(35) Kedmi, M.; Beaudet, A. L.; Orr-Urtreger, A. *Physiol. Genomics* **2004**, *17*, 221–229.

(36) Salas, R.; Pieri, F.; De Biasi, M. *J. Neurosci.* **2004**, *24*, 10035–10039.

(37) Carroll, F, I.; Hu, X.; Navarro, H. N.; Deschamps, J.; Abdrakhmanova, G. R.; Damaj, M. I.; Martin, B. R. *J. Med. Chem.* **2006**, *49*, 3244–3250.

(38) Kanne, D. B.; Tomizawa, M.; Durkin, K. A.; Casida, J. E. *Bioorg. Med. Chem. Lett.* **2005**, *15*, 877–881.

(39) Pabreza, L. A.; Dhawan, S.; Kellar, K. J. *Mol. Pharmacol.* **1991**, *39*, 9–12.

(40) Astles, P. C.; Baker, S. R.; Boot, J. R.; Broad, L. M.; Dell, C. P.; Keenan, M. *Curr. Drug Targets: CNS Neurol. Disord.* **2002**, *1*, 337–348.

(41) Baker, S. R.; Cases, M.; Keenan, M.; Lewis, R. A.; Tan, P. *Tetrahedron Lett.* **2003**, *44*, 2995–2999.

(42) Broad, L. M.; Felthouse, C.; Zwart, R.; McPhie, G. I.; Pearson, K. H.; Craig, P. J.; Wallace, L.; Broadmore, R. J.; Boot, J. R.; Keenan, M.; Baker, S. R.; Sher, E. *Eur. J. Pharmacol.* **2002**, *452*, 137–144.

(43) Baker, S. R.; Boot, J.; Brunavs, M.; Dobson, D.; Green, R.; Hayhurst, L.; Keenan, M.; Wallace, L. *Bioorg. Med. Chem. Lett.* **2005**, *15*, 4727–4730.

(44) Dorff, P.; Gordon, J.; Heys, J. R.; Keith, R. A.; McCarthy, D. J.; Phillips, E.; Smith, M. A. World Patent, WO2005030778, 2005.

(45) Glennon, R. A.; Herndon, J. L.; Dukat, M. *Med. Chem. Res.* **1994**, *4*, 461–473.

(46) Glennon, R. A.; Dukat, M. *Bioorg. Med. Chem. Lett.* **2004**, *14*, 1841–1844.

(47) White, R.; Malpass, J. R.; Handa, S.; Baker, S. R.; Broad, L. M.; Folly, L.; Mogg, A. *Bioorg. Med. Chem. Lett.* **2006**, 5493–5497.

(48) Kellar, K. J.; Xiao, Y. In *Handbook of Contemporary Neuropharmacology*; Sibley, D. R., Hanin, I., Khar, M., Skolnick, P., Eds.; Wiley and Sons: New York, 2007; Chapter 4, pp 107–146.

(49) Bunnelle, W. H.; Dart, M. J.; Schrimpf, M. R. *Curr. Top. Med. Chem.* **2004**, *4*, 299–334.